NASA/TM—2002–211546

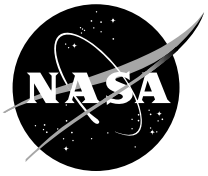

Artificial Aging Effects on Cryogenic Fracture Toughness of the Main Structural Alloy for the Super Lightweight Tank

P.S. Chen
IIT Research Institute, Huntsville, Alabama

W.P. Stanton
Marshall Space Flight Center, Marshall Space Flight Center, Alabama

February 2002

The NASA STI Program Office…in Profile

Since its founding, NASA has been dedicated to the advancement of aeronautics and space science. The NASA Scientific and Technical Information (STI) Program Office plays a key part in helping NASA maintain this important role.

The NASA STI Program Office is operated by Langley Research Center, the lead center for NASA's scientific and technical information. The NASA STI Program Office provides access to the NASA STI Database, the largest collection of aeronautical and space science STI in the world. The Program Office is also NASA's institutional mechanism for disseminating the results of its research and development activities. These results are published by NASA in the NASA STI Report Series, which includes the following report types:

- TECHNICAL PUBLICATION. Reports of completed research or a major significant phase of research that present the results of NASA programs and include extensive data or theoretical analysis. Includes compilations of significant scientific and technical data and information deemed to be of continuing reference value. NASA's counterpart of peer-reviewed formal professional papers but has less stringent limitations on manuscript length and extent of graphic presentations.

- TECHNICAL MEMORANDUM. Scientific and technical findings that are preliminary or of specialized interest, e.g., quick release reports, working papers, and bibliographies that contain minimal annotation. Does not contain extensive analysis.

- CONTRACTOR REPORT. Scientific and technical findings by NASA-sponsored contractors and grantees.

- CONFERENCE PUBLICATION. Collected papers from scientific and technical conferences, symposia, seminars, or other meetings sponsored or cosponsored by NASA.

- SPECIAL PUBLICATION. Scientific, technical, or historical information from NASA programs, projects, and mission, often concerned with subjects having substantial public interest.

- TECHNICAL TRANSLATION. English-language translations of foreign scientific and technical material pertinent to NASA's mission.

Specialized services that complement the STI Program Office's diverse offerings include creating custom thesauri, building customized databases, organizing and publishing research results…even providing videos.

For more information about the NASA STI Program Office, see the following:

- Access the NASA STI Program Home Page at ***http://www.sti.nasa.gov***

- E-mail your question via the Internet to help@sti.nasa.gov

- Fax your question to the NASA Access Help Desk at (301) 621–0134

- Telephone the NASA Access Help Desk at (301) 621–0390

- Write to:
  NASA Access Help Desk
  NASA Center for AeroSpace Information
  7121 Standard Drive
  Hanover, MD 21076–1320

NASA/TM—2002–211546

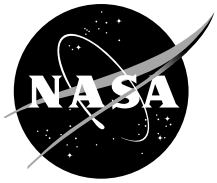

Artificial Aging Effects on Cryogenic Fracture Toughness of the Main Structural Alloy for the Super Lightweight Tank

P.S. Chen
IIT Research Institute, Huntsville, Alabama

W.P. Stanton
Marshall Space Flight Center, Marshall Space Flight Center, Alabama

National Aeronautics and
Space Administration

Marshall Space Flight Center • MSFC, Alabama 35812

February 2002

TRADEMARKS

Trade names and trademarks are used in this report for identification only. This usage does not constitute an official endorsement, either expressed or implied, by the National Aeronautics and Space Administration.

Available from:

NASA Center for AeroSpace Information
7121 Standard Drive
Hanover, MD 21076–1320
(301) 621–0390

National Technical Information Service
5285 Port Royal Road
Springfield, VA 22161
(703) 487–4650

TABLE OF CONTENTS

LIST OF FIGURES

LIST OF TABLES

LIST OF ACROYNMS, SYMBOLS, AND ABBREVIATIONS

%El	percent elongation (ductility)
Ag	silver
Al	aluminum
CFT	cryogenic fracture toughness
Cu	copper
FTR	fracture toughness ratio
ksi	thousand pounds per square inch
Li	lithium
LN_2	liquid nitrogen
Mg	magnesium
MSRC	multistep heating rate controlled (aging treatment)
NASA	National Aeronautics and Space Administration
SCC	stress corrosion cracking
SLWT	super lightweight tank
TEM	transmission electron microscopy
UTS	ultimate tensile strength
YS	yield strength

NOMENCLATURE

$\sqrt{\text{in}}$	square root inch
a	factor includes vibration frequency of atoms and area of critical nucleus
A_1	constant
A_2	constant
C_1	concentration of nucleation sites per unit volume
HR_B	Rockwell hardness B scale
k	Boltzmann's constant
K_{IC}	fracture toughness
L	longitudinal direction (orientation)
LT	longitudinal transverse direction (orientation)
N_{het}	heterogeneous nucleation rate
r	radius of the embryo
r_0	critical radius
ST	short transverse direction (orientation)
T	temperature (0 K)
T_1	strengthening precipitate
ΔG^*	activation energy barrier required to form critical-sized nuclei
ΔG_m	free energy of strain due to formation of precipitate particle
ΔG_M	activation energy for atomic migration
ΔG_{r_0}	energy required to form critical embryo
ΔG_S	surface free energy
ΔG_V	volume free energy
θ'	Al_2Cu precipitate
θ''	Al_2Cu precipitate (a precursor of θ')
ω	factor that includes vibration frequency of atoms and area of critical nucleus

TECHNICAL MEMORANDUM

ARTIFICIAL AGING EFFECTS ON CRYOGENIC FRACTURE TOUGHNESS OF THE MAIN STRUCTURAL ALLOY FOR THE SUPER LIGHTWEIGHT TANK

1. INTRODUCTION

NASA initiated research to increase payload weight capacity for the Space Shuttle, in order to support deployment of the *International Space Station* in a cost-effective manner. Aluminum-copper-lithium (Al-Cu-Li) alloys are considered ideal for this launch system, since they combine high strength with low density compared to other Al-based alloys; e.g., alloys 2219 and 2014, traditionally used in aerospace applications. The external tank was fabricated from alloy 2219. It has been replaced with a super lightweight tank (SLWT) fabricated from large rolled plates of an Al-Cu-Li alloy (alloy 2195).

Cryogenic strength and fracture toughness are critical to this application, since the SLWT houses liquid oxygen and hydrogen. If properly processed and heat treated, this alloy can display higher fracture toughness at cryogenic than at ambient temperature. However, the properties of production materials have shown greater variation than those of established alloys, as is the case with any new alloy transitioned to a demanding application. To ensure proper quality control, NASA has imposed lot acceptance testing on alloy 2195 plate before it can be used in the SLWT program. To be accepted, materials must pass tensile, simulated service fracture, and stress corrosion cracking (SCC) tests. Simulated service fracture tests are conducted at cryogenic temperatures, while tensile and SCC tests are conducted at ambient temperatures. One lot acceptance guideline is that alloy 2195 must have a cryogenic fracture toughness (CFT) value >30 ksi$\sqrt{\text{in}}$. It is equally important that the alloy meet these requirements under simulated service conditions to enhance flight safety. Using these criteria, some commercial alloy 2195 heats were rejected for the SLWT program because they failed to meet simulated service fracture requirements.

Previous studies have shown that CFT was significantly improved in alloy 2195 by a multistep heating rate controlled (MSRC) aging treatment which was developed in-house.[1,2] However, MSRC aging requires very tight temperature controls that cannot be readily applied in a production environment, which uses large-scale furnaces that are unable to maintain the designed heating rate of 0.6 °C (1 °F)/hr and may fluctuate by at least ±3 °C (5 °F) to the desired aging temperatures.

A new program was initiated to determine whether the MSRC aging treatment could be further modified to facilitate its implementation to flight hardware production. It was successfully redesigned as a simplified two-step aging treatment. The new treatment can control the size and location of strengthening precipitate T_1 in the same way as MSRC aging, thus achieving higher properties at cryogenic temperatures. When tested on several materials that were previously rejected for the SLWT program, two-step aging proved to be so effective that the improved CFT properties actually exceeded the simulated service fracture requirements. Ultimately, it is hoped that the two-step aging treatment can be

exploited to reduce the rejection rate of low-property materials, making the SLWT program more cost effective. This Technical Memorandum details the effects of the two-step aging treatment.

2. TECHNICAL APPROACH

This study used an alloy which had yield strength (YS) >73 ksi and displayed a cryogenic-to-ambient fracture toughness ratio (FTR) <1 after isothermal aging.[1,2] In Al-Cu-Li alloys, FTR correlates well with the size and density of T_1 in the matrix[2] (see fig. 1). High CFT can be achieved by suppressing T_1 precipitation at subgrain boundaries and enhancing T_1 nucleation in the matrix, thus eliminating premature fractures along precipitate-rich subgrain boundaries (see fig. 2).

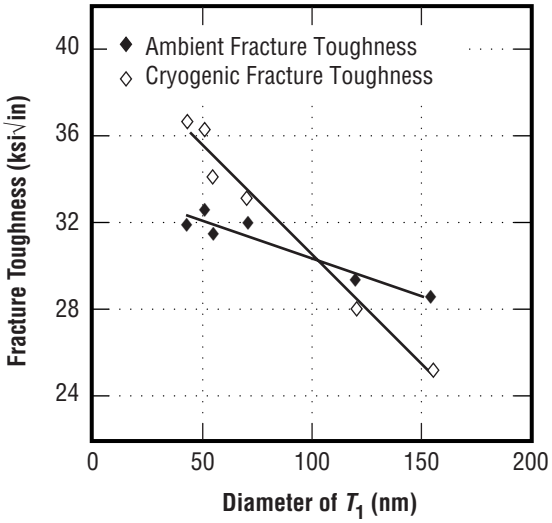

Figure 1. Fracture toughness versus maximum size of T_1 at subgrain boundaries, with fracture toughness decreasing as T_1 size increases.[1,2]

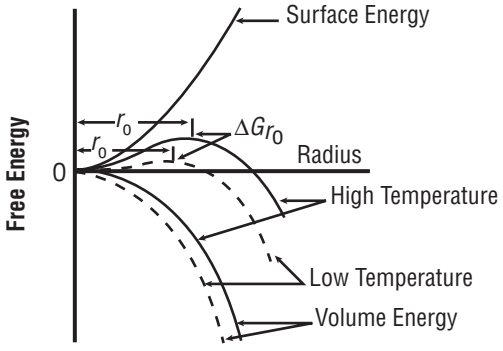

Figure 2. Effects of precipitation temperature on free energy of a precipitate particle as a function of its radius.[3]

In Al-Cu-Li alloys, T_1 particles generally precipitate heterogeneously on matrix dislocations and/or subgrain boundaries, depending on aging temperatures and duration.[4] In alloy 2095 (which is similar to alloy 2195), lower aging temperature was found to suppress T_1 precipitation at subgrain boundaries,[4] explained on the basis of equation (1) for the heterogeneous nucleation rate (N_{het}):[5]

$$N_{\text{het}} = \omega C_1 \exp\left(\frac{-\Delta G_M}{kT}\right) \cdot \left(\frac{-\Delta G^*}{kT}\right) \text{nuclei m}^{-3}\text{s}^{-1} \quad , \tag{1}$$

where

N_{het} = Heterogeneous nucleation rate

ω = A factor that includes vibration frequency of atoms and area of critical nucleus

C_1 = Concentration of nucleation sites per unit volume

ΔG_M = Activation energy for atomic migration

ΔG^* = Activation energy barrier required to form critical-sized nuclei

k = Boltzmann's constant

T = Temperature (0 K).

When the alloy composition is fixed, this equation indicates that the heterogeneous nucleation rate is greatly dependent on C_1 and ΔG^*. Arranged in decreasing order, ΔG^* indicates (1) homogeneous sites, (2) vacancies, (3) dislocations, (4) stacking faults, (5) grain boundaries and interphase boundaries, and (6) free surfaces.

Apparently, alloy 2195 requires more activation energy for T_1 nucleation on matrix dislocations than on subgrain boundaries. However, matrix nucleation sites generally outnumber subgrain boundary sites, especially when the alloy is stretched prior to aging. With low undercooling (high activation barrier/high aging temperature), nucleation rates will be highest at sites requiring little activation energy, such as grain and subgrain boundaries. As undercooling increases (low activation barrier/low aging temperature), higher nucleation rates are seen at sites that have the highest concentration of nucleation sites. Therefore, by lowering the aging temperature, matrix dislocations become favorable nucleation sites and T_1 nucleation can be restrained at subgrain boundaries.

However, low-temperature aging is associated with sluggish aging kinetics, which are not desirable for industrial production. Furthermore, it was not clear whether a low aging temperature could sufficiently strengthen the alloy while improving its fracture toughness. Therefore, a need existed to develop a new aging treatment that could improve CFT while retaining YS at 75–78 ksi and aging up the properties within a reasonable length of time.

Precipitation of strengthening phases requires a free-energy change of the system, as expressed in equation (2):[3]

$$\Delta G = -\Delta G_V + \Delta G_S + \Delta G_m \quad , \tag{2}$$

where

ΔG_V = Volume free energy

ΔG_S = Surface free energy

ΔG_m = Free energy of strain due to formation of precipitate particle.

The ΔG_S varies with the area of the particle, while ΔG_V varies with the volume of the particle. Therefore, assuming a spherical particle and $\Delta G_m = 0$, equation (2) may be written as

$$\Delta G = -A_1 r^3 + A_2 r^3 \quad , \tag{3}$$

where

A_1 and A_2 = Constants

r = Radius of the embryo.

Figure 2 is a plot of equation (3). The total free energy is positive when the particle radius is small, since the ΔG_S is larger than the ΔG_V. However, the total free energy becomes negative as the radius increases.

A particle with a radius less than the critical radius (r_0) tends to dissolve in the solid solution, while a particle with a radius larger than r_0 tends to grow continuously because the free energy is reduced as it grows. The size of a stable nucleus (r_0) varies with temperature. As the temperature is lowered, the r_0 for precipitate nucleation rapidly decreases in size, as does the energy necessary to form this critical embryo (ΔG_{r_0}). Therefore, decreasing temperature correlates with an increase in the total number of embryos that can precipitate.

Based on this theory, an MSRC aging treatment[1,2] was developed to promote T_1 nucleation and growth in the matrix rather than at subgrain boundaries (see table 1). Aging began with initial holding at low temperature with high undercooling, in order to enhance formation of T_1 nuclei in the matrix; then the furnace temperature was gradually increased 0.6 °C (1 °F)/hr to permit each precipitate nuclei to grow above the r_0 and become a stable nucleus. These nuclei continued to grow during aging, with negligible dissolution into solid solution. In addition, long-term aging at low temperatures allowed T_1 precipitates to grow in the matrix before they could nucleate and grow at the subgrain boundaries.

As temperatures continued to rise, T_1 eventually nucleated at subgrain boundaries and began to grow. However, this treatment reduced time at the highest aging temperature. Thus, T_1 was permitted to nucleate and grow in the matrix before precipitation occurred at the subgrain boundaries. Early growth of T_1 in the matrix greatly reduced Cu and Li concentrations adjacent to the subgrain boundaries, hindering the growth of subgrain boundary T_1. At the subgrain boundaries, T_1 was smaller and scarcer than that seen in alloy 2195 subjected to isothermal aging.

Table 1. Five-step aging treatments.

Aging Treatment No.	132 °C (270 °F) (hr)	135 °C (275 °F) (hr)	138 °C (280 °F) (hr)	141 °C (285 °F) (hr)	143 °C (290 °F) (hr)
1	5	5	5	5	5
2	5	10	10	10	10
3	5	15	15	15	15
4	5	20	20	20	20
5	10	5	10	15	20
6	10	10	5	20	15
7	10	15	20	5	10
8	10	20	15	10	5
9	15	5	15	20	10
10	15	10	20	15	5
11	15	15	5	10	15
12	15	20	10	5	20
13	20	5	20	10	15
14	20	10	15	5	20
15	20	15	10	20	5
16	20	20	5	15	10

In order to redesign and simplify MSRC aging, a new aging process had to be able to nucleate and grow T_1 in the same way. Therefore, the approach began with a series of five-step aging treatments that resembled MSRC aging (table 1). Based on test results and microstructural characterization, promising five-step aging treatments were selected and converted into simplified three- and two-step aging processes (table 2). The most promising two-step aging treatment (No. 24) was selected for tensile and cryogenic properties evaluation. This treatment was significant in that it achieved high cryogenic properties in the same manner as the more sophisticated MSRC aging.

Table 2. Three- and two-step aging treatments.

Aging Treatment No.	129 °C (270 °F) (hr)	132 °C (270 °F) (hr)	135 °C (275 °F) (hr)	138 °C (280 °F) (hr)	141 °C (285 °F) (hr)	143 °C (290 °F) (hr)
17	–	20	–	20	–	15
18	–	20	–	20	–	10
19	–	20	–	20	–	5
20	–	20	–	15	–	10
21	–	15	–	20	–	10
22	–	15	–	15	–	10
23	20	–	20	–	20	–
24	–	20	–	40	–	–
25	–	–	20	–	40	–

3. EXPERIMENTAL PROCEDURES

Alloy 2195 (nominal composition: Al-4.0Cu-1.0Li-0.52Mg-0.42Ag-0.12Zr) was received in the form of 1.7-in-thick rolled plates, which were solutionized and stretched 3 percent at ambient temperature. The following procedures were then performed:

(1) Tensile tests were carried out at ambient temperature, using flat tensile specimens to evaluate the effects of microstructural variation through the plate thickness. Uniaxial tensile properties were evaluated in the longitudinal (*L*), longitudinal transverse (*LT*), and short transverse (*ST*) directions, with at least two tests performed in each orientation. Fracture toughness tests were performed at ambient temperature and –196 °C (–320 °F). The plates were evaluated with the notch parallel to the rolling direction orientation per American Society for Testing Materials specification E740. The specimens were fatigue-precracked at 20 Hz, then tensile tested to failure at a crosshead speed of 0.13 cm/min. Precrack length and maximum load-to-failure were factored into the standard equation. Simulated service tests were performed at –196 °C (–320 °F).

(2) Microstructural characterization was performed using a JEOL, Ltd. 2000F transmission electron microscope operated at 200 kV. Samples were jet polished in an electrolyte (70-percent methanol and 30-percent nitric acid) at –20 °C (–4 °F) with an applied potential of 12 V. Precipitates were examined using selected area diffraction as well as bright and dark field imaging techniques. Matrix and subgrain boundary precipitates were examined using a beam direction near the $[110]_{matrix}$ zone axis. Two T_1 variants and one Al_2Cu precipitate (θ′) (or Al_2Cu precipitate—a precursor of θ′ (θ″)) variant were oriented edge-on to the beam, so that their size and distribution could be readily determined.

4. RESULTS

4.1 Hardness and Microstructure

Table 3 shows hardness variation as a result of the five-step aging treatment. The alloy was underaged at 132 °C (270 °F) to enhance precipitate nucleation in the matrix, and then heated to 135, 138, 141, and 143 °C (275, 280, 285, and 290 °F, respectively) for various times in an effort to obtain a peak or near-peak aged condition, while preventing preferential nucleation and growth of T_1 at subgrain boundaries. For alloy 2195, a hardness of 90 to 91 Rockwell hardness B scale (HR_B) is roughly equivalent to 73 ksi YS in the *L* and *LT* directions (the minimum strength requirement for this alloy). Among the five-step aging treatments, 13 of 16 treatments achieved a minimum hardness of 90 HR_B, with Nos. 4, 7, 15, and 16 reaching a minimum hardness of 91 HR_B even before being aged at 143 °C (290 °F) (see table 3). More importantly, Nos. 8, 14, and 15 reached a hardness of ≈87 HR_B after the third step at 138 °C (280 °F), indicating that the required hardness of 91 HR_B could be achieved without having to age the material at temperatures above 138 °C (280 °F).

Table 3. Five-step aging hardness values for rejected lot of alloy 2195 (lot 950M029B).

Aging Treatment No.	132 °C (270 °F) (hr)	HR_B	135 °C (275 °F) (hr)	HR_B	138 °C (280 °F) (hr)	HR_B	141 °C (285 °F) (hr)	HR_B	143 °C (290 °F) (hr)	HR_B
1	5	67.16	5	71.1	5	74.2	5	78.02	5	79.08
2	5	67.16	10	75.86	10	75.86	10	85.48	10	85.66
3	5	67.16	15	79	15	80	15	89	15	90.5
4	5	67.16	20	79.5	20	82.6	20	91.9	20	92.2
5	10	72.2	5	75.8	10	78.8	15	87.9	20	91.2
6	10	72.2	10	76.8	5	79.4	20	89.2	15	91.4
7	10	72.2	15	82.2	20	84.8	5	91.6	10	89.8
8	10	72.2	20	82.7	15	86.6	10	87.5	5	89.4
9	15	73.2	5	76.8	15	82.1	20	89.3	10	90.8
10	15	73.2	10	79.8	20	83.2	15	89.4	5	90.2
11	15	73.2	15	81.4	5	82.5	10	83.2	15	91.3
12	15	73.2	20	79.4	10	84.5	5	85.6	20	90.5
13	20	76.2	5	77.2	20	82.3	10	87.4	15	91.2
14	20	76.2	10	79.1	15	87.1	5	88.2	20	91.5
15	20	76.2	15	80.2	10	83.4	20	91.2	5	92.2
16	20	76.2	20	81.4	5	87.4	15	91.5	10	90.8

In order to determine whether five-step aging could be further simplified, several aging treatments were conducted with three steps (Nos. 17 to 23) and two steps (Nos. 24 and 25) (see table 4). Among the three-step aging treatments, No. 17 reached a hardness of 91.7 HR_B after 55 hr. Promising results were also obtained for a two-step aging treatment (No. 24) which achieved a hardness of more than 90 HR_B after being aged at 132 °C (270 °F)/20 hr followed by 138 °C (280 °F)/40 hr. These results proved that an appropriate combination of temperature and time would permit five aging steps to be reduced to three or two steps.

Table 4. Three- and two-step aging hardness values for rejected lot of alloy 2195 (lot 950M029B).

Aging Treatment No.	129 °C (265 °F) (hr)	HR_B	132 °C (270 °F) (hr)	HR_B	135 °C (275 °F) (hr)	HR_B	138 °C (280 °F) (hr)	HR_B	141 °C (285 °F) (hr)	HR_B	143 °C (290 °F) (hr)	HR_B
17	–	–	20	76.2	–	–	20	86.2	–	–	15	91.7
18	–	–	20	–	–	–	20	–	–	–	10	88.9
19	–	–	20	–	–	–	20	–	–	–	5	87.1
20	–	–	20	–	–	–	15	84.1	–	–	10	88.0
21	–	–	15	–	–	–	20	84.4	–	–	10	88.5
22	–	–	15	–	–	–	15	–	–	–	10	87.6
23	20	75.8	–	–	20	83.2	–	–	20	89.2	–	–
24	–	–	20	76.2	–	–	40	90.7	–	–	–	–
25	–	–	–	–	20	79.1	–	–	40	89.8	–	–

Transmission electron microscopy (TEM) was used to examine the step-aged microstructures. After aging at 132 °C (270 °F)/20 hr, the matrix consisted of numerous fine θ″, with scattered T_1 (see fig. 3(a)). The large number of very fine θ″ indicated that an early stage of nucleation had taken place at 132 °C (270 °F). TEM diffraction using a $[110]_{Al}$ zone axis confirmed the observation that aging at 132 °C (270 °F) resulted in very early stage precipitation of T_1 (see fig. 3(b)). Moderate growth of both θ″ and T_1 occurred after additional aging at 135 °C (275 °F) (see fig. 4(a)). At this stage, the subgrain boundaries were still decorated with pile-up dislocations, with no sign of preferential T_1 precipitation. Aging at 135 °C (275 °F) enhanced T_1 nucleation and growth in the matrix instead of the subgrain boundaries (see fig. 4(b)).

At 138 °C (280 °F), T_1 grew considerably, but the matrix still contained a large number of θ″ precipitates (see fig. 5(a)). More significant T_1 growth occurred at subgrain boundaries after aging at 141 °C (285 °F) (see fig. 5(b)). After final step-aging at 143 °C (290 °F), hardness increased rapidly, indicating near-peak precipitation of the strengthening phases. T_1 was the majority phase in the matrix and was present at subgrain boundaries in sizes no coarser than the matrix T_1 (see fig. 6). Similar microstructural evolution was observed in the three- and two-step aging treatments. Figure 7 shows the microstructure that resulted from two-step aging (No. 24). The similarity in final microstructure between Nos. 4 and 24 indicated that two-step aging could be used to achieve the same precipitate nucleation and growth characteristics observed during five-step aging.

Substantial microstructural differences were found between conventionally aged and step-aged materials. In conventionally aged alloy, T_1 was coarser and had a much higher density in the subgrain boundaries than in the matrix.[1,2] In step-aged alloy, the subgrain boundaries were mostly devoid of T_1 (see fig. 7). Whereas T_1 occasionally existed at subgrain boundaries, it was not as dense as T_1 in the matrix. Differences also existed in the size and density of matrix precipitates. Conventionally aged alloy contained more T_1 than θ′ and θ″ in the matrix, while two-step aging produced more θ′ and θ″ than T_1 in the matrix. This finding clearly indicates that two-step aging can achieve the same strength levels as conventional aging, by precipitating more θ′ and θ″ in the matrix, while preventing preferential T_1 precipitation at subgrain boundaries.

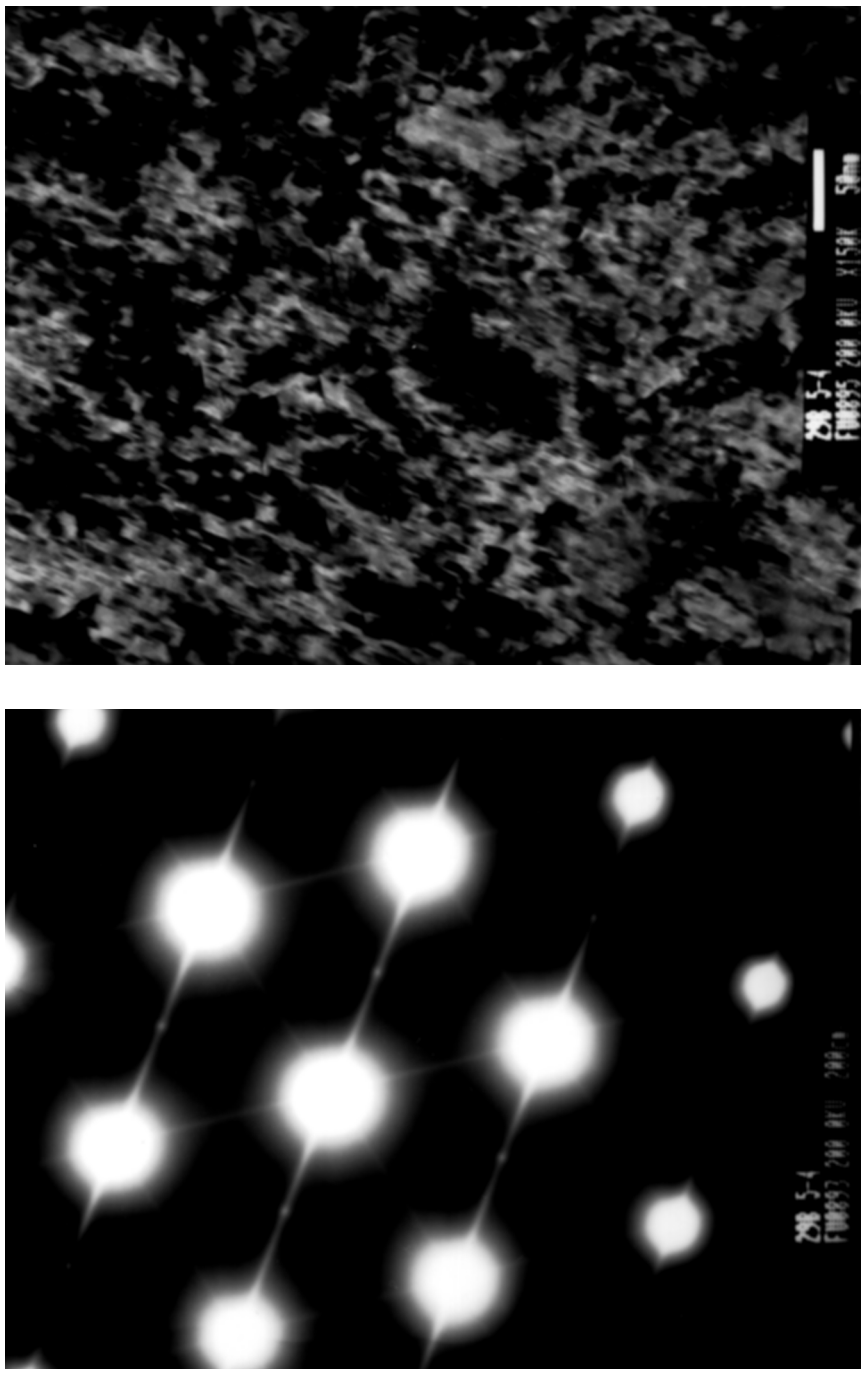

(a)

(b)

Figure 3. Precipitate morphology after preliminary step-aging at 132 °C (270 °F)/20 hr. TEM photographs showing: (a) early stage of precipitate nucleation growth in the matrix and (b) diffraction pattern with strong streakings, indicating early nucleation and precipitate growth.

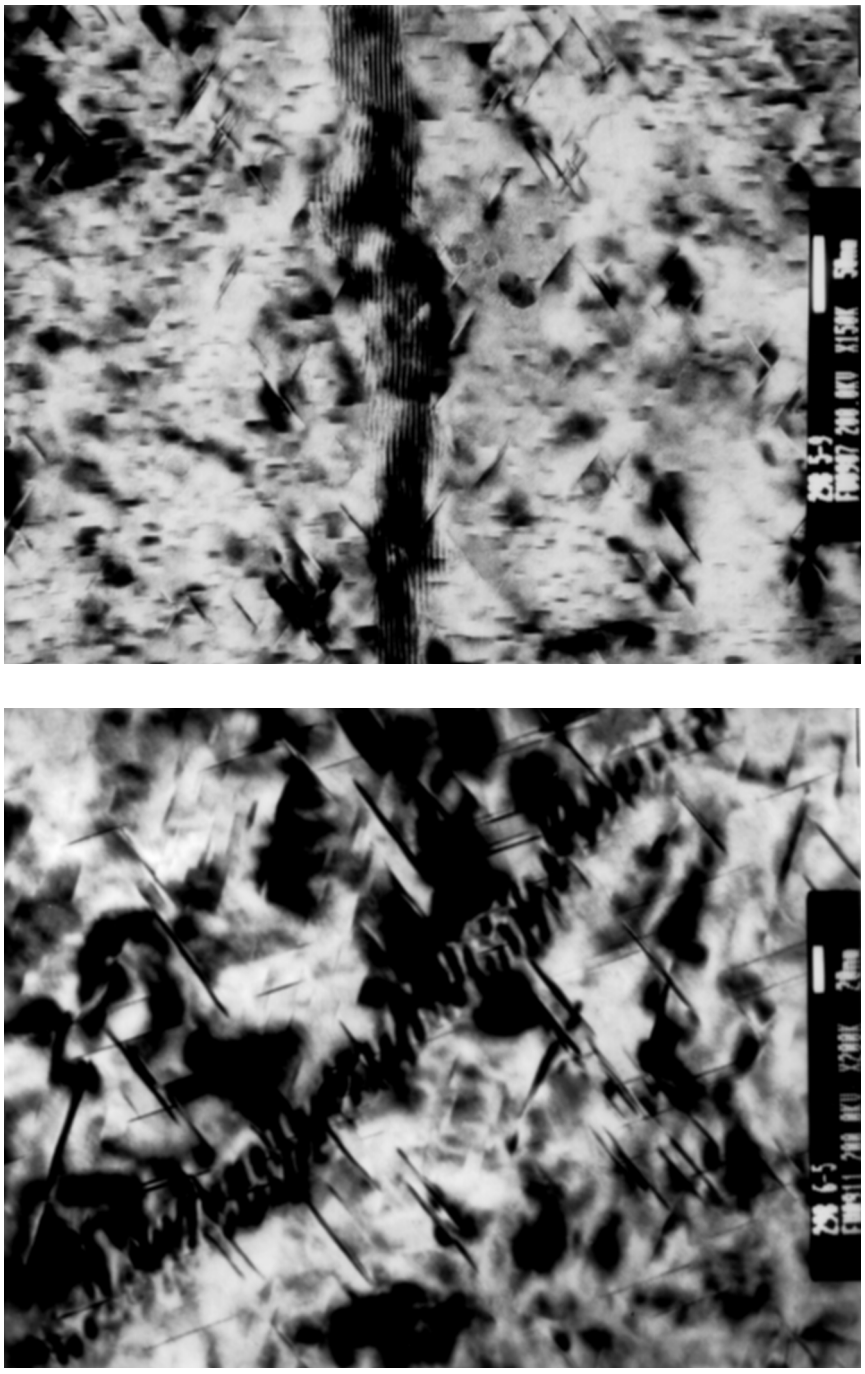

(a)

(b)

Figure 4. Early stage of T_1 growth: (a) on matrix during 132 °C (270 °F)/ 20 hr + 135 °C (275 °F)/10 hr (No. 14) and (b) at subgrain boundaries during 132 °C (270 °F)/20 hr + 135 °C (275 °F)/ 20 hr (No. 16).

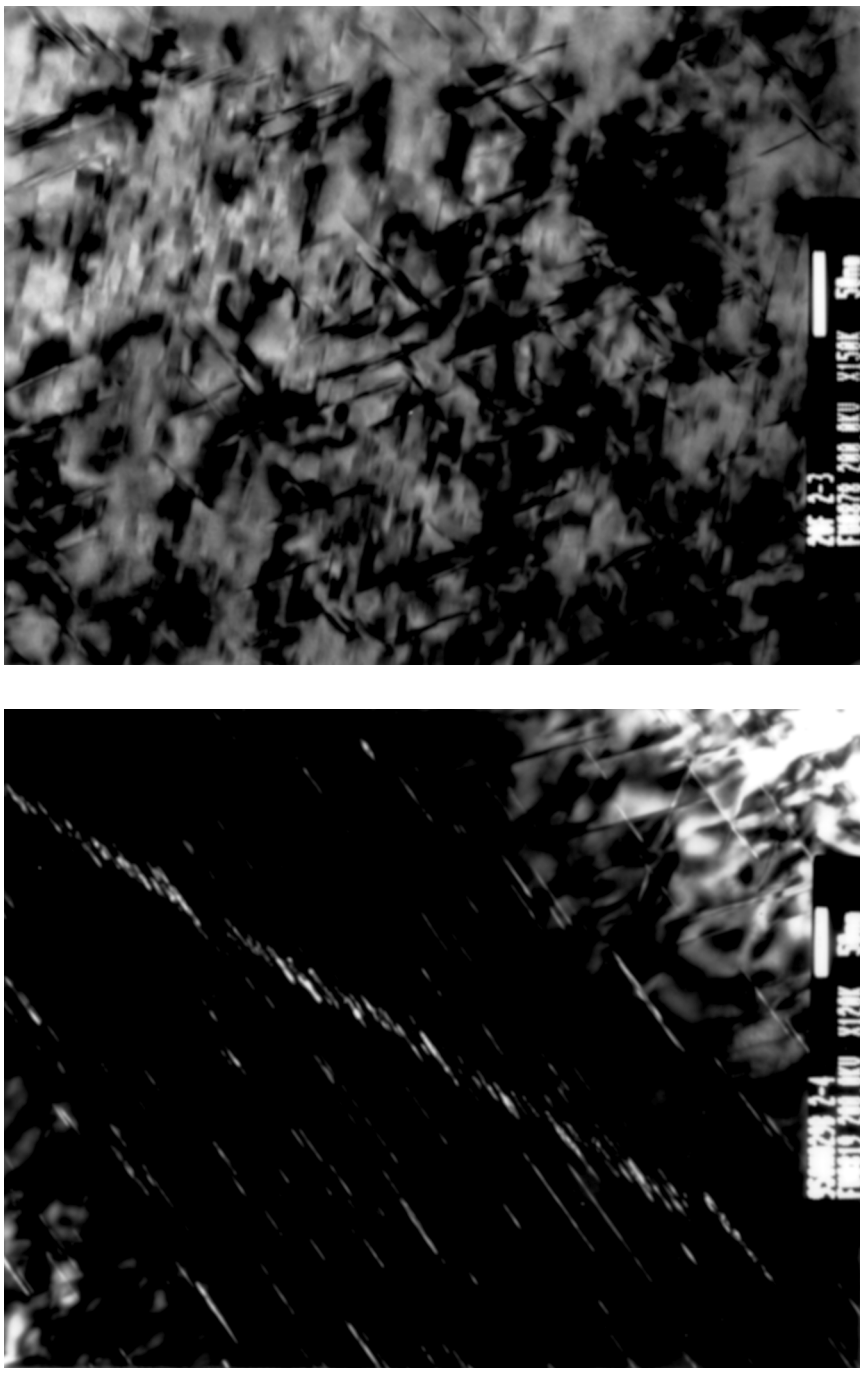

(a)

(b)

Figure 5. Noticeable T_1 growth during different five-step aging treatments. TEM photographs showing: (a) early stage in matrix during 132 °C (270 °F)/20 hr + 135 °C (275 °F)/20 hr (No. 16) and (b) more T_1 growth at subgrain boundaries during 132 °C (270 °F)/5 hr +135 °C (275 °F)/20 hr + 138 °C (280 °F)/20 hr + 141 °C (285 °F)/20 hr (No. 4).

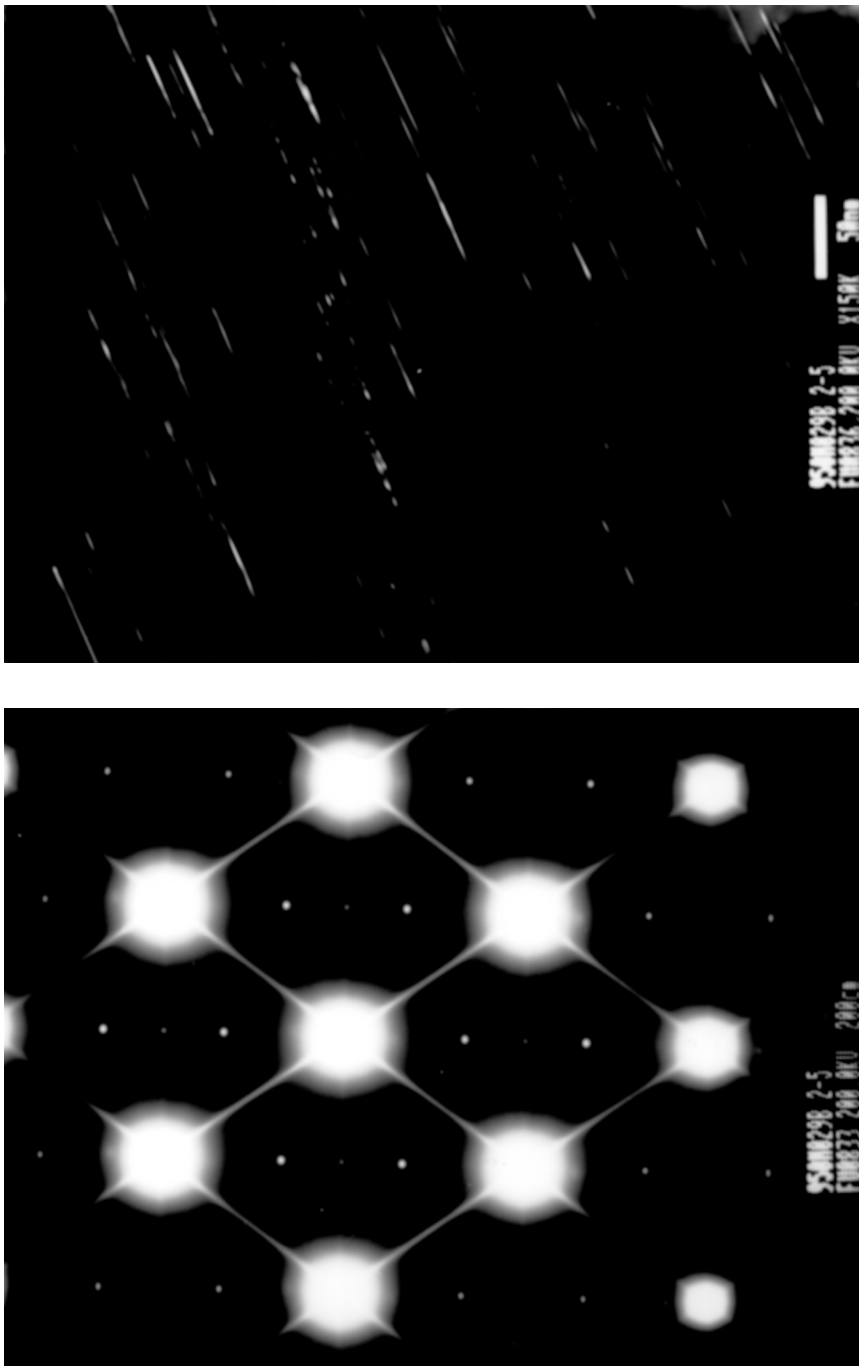

Figure 6. Significant T_1 growth during five-step aging treatment. TEM photographs showing: (a) 132 °C (270 °F)/5 hr + 135 °C (275 °F)/20 hr + 138 °C (280 °F)/20 hr + 141 °C (285 °F)/20 hr + 143 °C (290 °F)/20 hr (No. 4) and (b) TEM diffraction pattern.

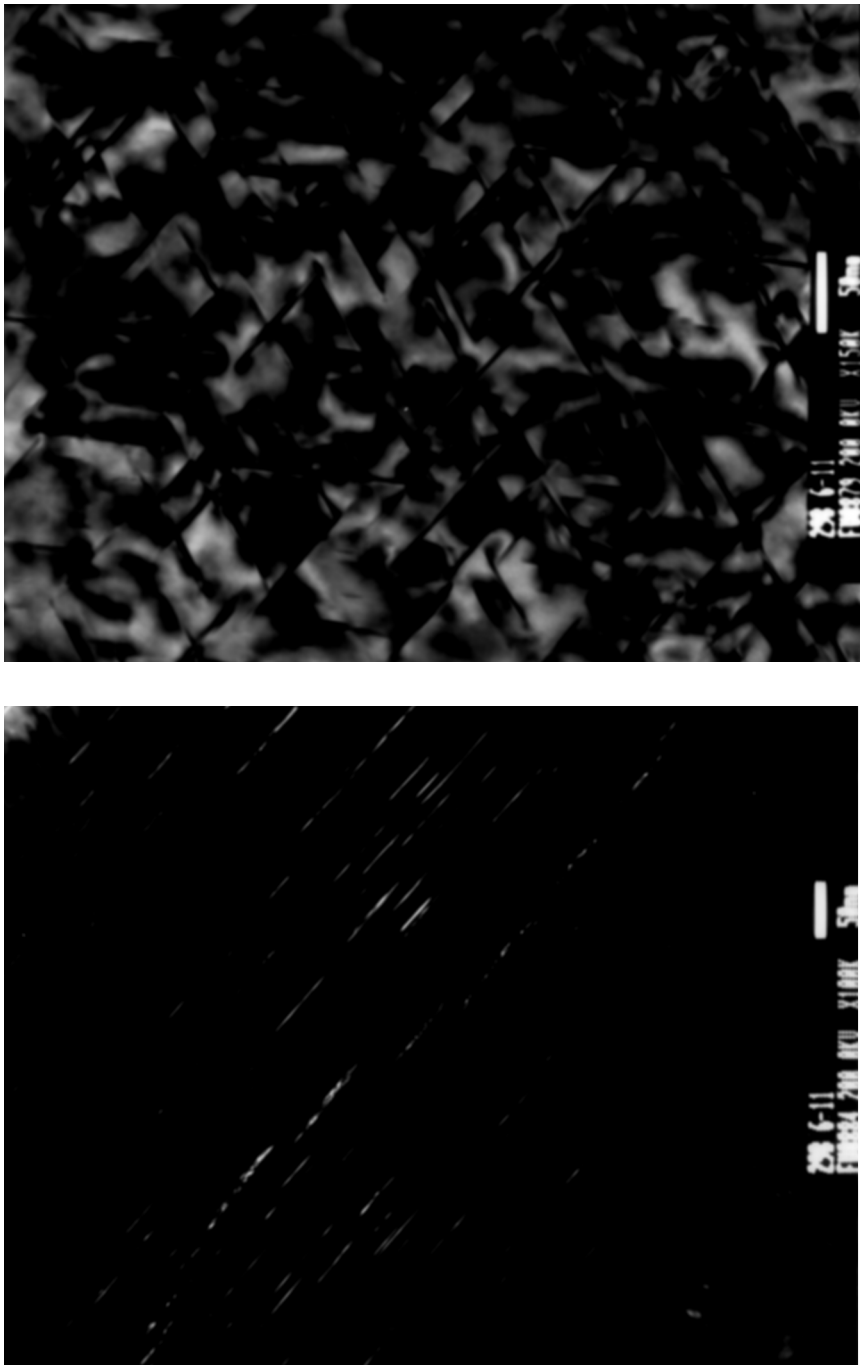

(a)

(b)

Figure 7. Very limited T_1 growth after two-step aging treatment at 132 °C (270 °F)/20 hr + 138 °C (280 °F)/40 hr (No. 24). TEM photographs showing: (a) matrix and (b) subgrain boundaries.

4.2 Mechanical Properties

Several step-aging treatments (Nos. 17, 24, and 25) were selected for tensile strength and fracture toughness evaluation, since the SLWT program requires a minimum YS of 73 ksi in the *L* direction. Tensile data indicated that the two-step aging can achieve the same YS and ductility levels as those produced by conventional aging (see table 5). The most noticeable improvement was seen in CFT, for which the minimum requirement is 30 ksi√in (table 6). Two-step aging significantly improved CFT on a rejected lot (950M029B) (see table 6 and fig. 8—MSRC aging data[1,2] is included for comparison). The CFT was as low as 25.4 ksi√in for conventionally aged lot 950M029B (a bad lot), whereas two-step aging improved its CFT to ≈34 ksi√in (an improvement of over 30 percent). Two-step aging also improved the CFT for lot 950M020F (a good lot) by ≈10 percent.

Table 5. Tensile properties for aged alloy 2195.

Lot No.	Aging No.	Orientation	YS (ksi)	UTS (ksi)	%El
950M029B	17	*L*	77.4	80.9	8.5
		ST	70.3	83.4	5.5
950M020F	17	*L*	72.2	76.8	9.3
		ST	69.9	82.2	4.7
950M029B	24	*L*	79.4	84.5	9.5
		LT	76.8	84.6	9.9
		ST	69.6	82.2	4.5
950M020F	24	*L*	79.1	85.7	10.6
		LT	71.8	81.2	10.1
		ST	67.2	80.5	7.6
950M029B	25	*L*	77.4	81.1	9.0
		ST	71.8	84.1	4.8
950M020F	25	*L*	73.8	77.8	9.3
		ST	71.85	83.9	4.7

Table 6. Mechanical properties for aged alloy 2195.

Lot No. (3% Stretch)	Aging	YS (ksi)	UTS (ksi)	%El	K at *a*/2 (LN_2)	K at *a*/2 (Ambient)
950M029B	MSRC [1]	77.8	85.1	9.4	32.10	31.80
	two-step aging No. 24	76.8	84.6	9.9	33.74	30.44
	Conventional [1]	74.0	83.1	7.0	25.40	30.04
950M020F	MSRC [1]	76.1	83.0	9.1	37.13	34.50
	two-step aging No. 24	71.8	81.3	10.0	37.64	34.79
	Conventional [1]	76.1	83.4	8.0	34.91	32.90

MSRC [1]: Denotes heating rate-controlled aging process.

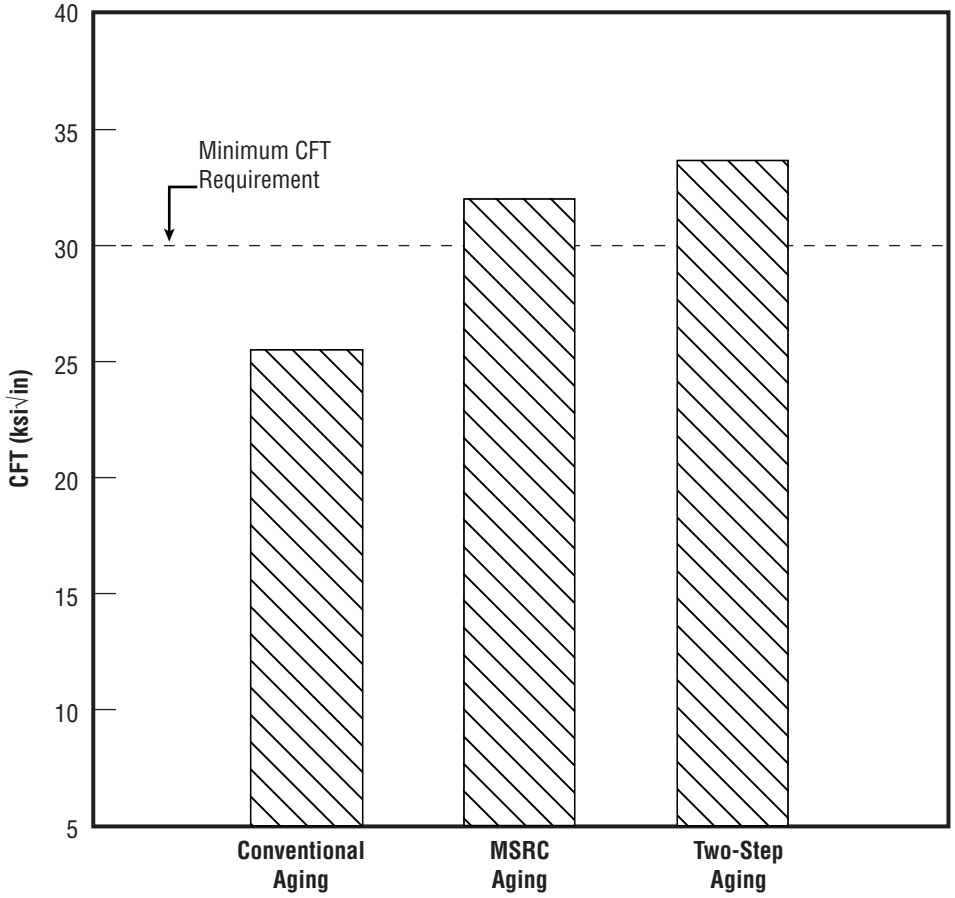

Figure 8. Comparative data indicating that two-step (No. 24) and MSRC aging greatly improved CFT to meet minimum fracture toughness requirement (30 ksi√ in).

Compared with conventional aging, both MSRC and two-step (No. 24) aging offered considerable improvements in fracture toughness that ranged from 10 to 30 percent, depending upon the original CFT. A simulated service test was conducted using lot 950M029B, which had failed to pass when aged conventionally. After two-step aging, lot 950M029B passed by a very comfortable margin, as well as exhibiting much higher fracture toughness at cryogenic than at ambient temperature (table 7).

Table 7. Simulated service test results for alloy 2195 (lot 950M029B) that received two-step aging (No. 24).

Test Type, Temperature (°F)	Proof Stress (ksi)	Fracture Stress (ksi)	K_{IC} at *a*/2 (ksi√in)
Proof, Ambient	–	76.25	30.57
SS, –323	74.10	85.07	34.11

4.3 Discussion

This study demonstrates that a special aging treatment can be designed to obtain a desirable microstructure for alloy 2195, resulting in much improved CFT. The major factors that affect CFT are matrix and subgrain boundary precipitates, especially T_1 at subgrain boundaries. In Al-Li alloys, improved CFT has been correlated to such factors as solidification of low-melting point impurities,[6] reduced strain localization in closer and more widely spaced slip bands,[7] increased homogeneity of plastic deformation from increased strain-hardening capacity,[8] and delaminated toughening on fracture surfaces.[9,10] However, these mechanisms are not responsible for the improvements observed in this study, because the alloy chemistry, thermomechanical processing, grain size, and YS do not exhibit distinguishable differences when specimens are made out of the same lot.

This study strongly suggests that, if preferential T_1 precipitation can be prevented at subgrain boundaries, alloy 2195 will have inherently higher fracture toughness at cryogenic than at ambient temperature. Subgrain boundary T_1 precipitation is probably the most important factor influencing CFT for alloy 2195. Since mechanical properties can be considerably impacted by any change in microstructure, excessive precipitation should be avoided in the subgrain boundaries of alloys intended for cryogenic applications.

The two-step aged specimen matrix has a microstructure that is significantly different from that of a conventionally aged specimen, producing much higher CFT with nearly the same YS. Similar YS levels were observed for the two-step and conventionally aged materials, which can be qualitatively correlated to microstructural characteristics; e.g., type, size, distribution, and density of strengthening phases T_1 and θ''. According to equation (1), the total number of embryos that can precipitate will increase as temperature decreases. Thus, the number of precipitate embryos is increased by initial holding at low temperature with high undercooling. Subsequent aging at 138 °C (280 °F) enables these embryos to grow slowly without dissolving, which increases the total number of precipitates. Therefore, additional strengthening is provided by the much higher number of θ' and θ'' precipitates present in two-step aged materials, producing YS comparable to conventionally aged materials. As aging continues, T_1 will eventually nucleate at subgrain boundaries and start to grow. However, this treatment allows T_1 to precipitate and grow in the matrix before the subgrain boundary. In addition, early coarsening of matrix T_1 greatly reduces the concentration of matrix Cu and Li, hindering the growth of subgrain boundary T_1 in a diluted Al-Cu-Li solid solution.

From an economical standpoint, two-step aging is not recommended for “good” lots, due to the fact that the aging duration (≈60 hr) is longer than conventional aging (≈30 to 35 hr). Instead, it should be exploited to process “bad” or marginal lots, in order to avoid material rejection due to low cryogenic properties. If implemented, the two-step aging treatment can improve SLWT reliability, decrease the rejection rate for low-property materials, and ultimately reduce NASA’s costs for this high-value material.

5. CONCLUSIONS

(1) The original MSRC aging treatment was successfully modified into a simplified two-step aging treatment that consists of 132 °C (270 °F)/20 hr + 138 °C (280 °F)/40 hr. Results indicated that two-step aging can achieve the same YS levels as those produced by conventional aging. Two-step aging was very effective at enhancing CFT and meeting simulated service requirements for previously rejected materials.

(2) The cryogenic properties were improved by controlling the size and location of T_1 precipitation in the same manner as MSRC aging. However, two-step aging reduced the length of time that the materials were exposed to high temperatures, thus constraining T_1 nucleation and growth at subgrain boundaries and permitting the material to achieve much improved CFT.

(3) During two-step aging, high tensile YS was achieved by promoting T_1 and θ'' nucleation in the matrix. The total density of T_1 and θ'' was higher than that seen in conventionally aged materials.

REFERENCES

1. Chen, P.S.; and Stanton, W.P.: "A New Aging Treatment for Improving Cryogenic Toughness of the Main Structural Alloy for the Super Lightweight Tank," *NASA Technical Memorandum 108524*, November 1996.

2. Chen, P.S.; Kuruvilla, A.K.; Malone, T.W.; et al.: "The Effects of Artificial Aging on the Microstructure and Fracture Toughness of Al-Cu-Li Alloy 2195," *Journal of Materials Engineering & Performance*, Vol. 7, p. 682, 1998.

3. Reed-Hill, R.E.: *Physical Metallurgy Principles*, Van Nostrand Reinhold, New York, NY, p. 368, 1973.

4. Blankenship, Jr., C.P.; and Starke, Jr., E.A.; "Structure-Property Relationships in Al-Li-Cu-Mg-Ag-Zr Alloy X2095," *Acta. Metall*., Vol. 42, p. 845, 1995.

5. Porter, D.A.; and Easterling, K.E.: *Phase Transformation in Metals and Alloys*, 2d ed., Chapman and Hall, U.K., p. 276, 1992.

6. Webster, D.: "The Effect of Low Melting Point Impurities on the Properties of Aluminum-Lithium Alloys," *Metall. Trans*., Vol. 18a, p. 2181, 1987.

7. Jata, K.V.; and Starke, Jr., E.A.: "Fracture Toughness of Al-Li-X Alloys at Ambient and Cryogenic Temperatures," *Script. Metall*., Vol. 22, p. 1553, 1988.

8. Glazer, J.; Verzasconi, S.L.; Sawtell, R.R.; et al.: "Mechanical Behavior of Aluminum-Lithium Alloys at Cryogenic Temperatures," *Metall. Trans*., Vol. 18a, p. 1695, 1987.

9. Xu, Y.B.; Wang, L.; Zhang, Y.; et al.: "Fatigue and Fracture Behavior of an Aluminum-Lithium Alloy 8090–T6 at Ambient and Cryogenic Temperature," *Metall. Trans*., Vol. 22a, p. 723, 1991.

10. Rao, K.T.V.; Yu, W.; and Ritchie, R.O.: "Cryogenic Toughness of Commercial Aluminum-Lithium Alloys: Role of Delamination Toughening," *Metall. Trans*., Vol. 20a, p. 485, 1989.

REPORT DOCUMENTATION PAGE

Form Approved
OMB No. 0704-0188

1. AGENCY USE ONLY *(Leave Blank)*	2. REPORT DATE	3. REPORT TYPE AND DATES COVERED
	February 2002	Technical Memorandum

4. TITLE AND SUBTITLE

Artificial Aging Effects on Cryogenic Fracture Toughness of the Main Structural Alloy for the Super Lightweight Tank

5. FUNDING NUMBERS

6. AUTHORS

P.S. Chen* and W.P. Stanton

7. PERFORMING ORGANIZATION NAMES(S) AND ADDRESS(ES)

George C. Marshall Space Flight Center
Marshall Space Flight Center, AL 35812

8. PERFORMING ORGANIZATION REPORT NUMBER

M–1041

9. SPONSORING/MONITORING AGENCY NAME(S) AND ADDRESS(ES)

National Aeronautics and Space Administration
Washington, DC 20546–0001

10. SPONSORING/MONITORING AGENCY REPORT NUMBER

NASA/TM—2002–211546

11. SUPPLEMENTARY NOTES

Prepared for Engineering Directorate, Materials, Processes, and Manufacturing Department
*IIT Research Institute, Huntsville, AL

12a. DISTRIBUTION/AVAILABILITY STATEMENT

Unclassified-Unlimited
Subject Category 26
Nonstandard Distribution

12b. DISTRIBUTION CODE

13. ABSTRACT *(Maximum 200 words)*

In 1996, Marshall Space Flight Center developed a multistep heating rate-controlled (MSRC) aging technique that significantly enhanced cryogenic fracture toughness (CFT) and reduced the statistical spread of fracture toughness values in alloy 2195 by controlling the location and size of strengthening precipitate T_1. However, it could not be readily applied to flight-related hardware production, primarily because large-scale production furnaces are unable to maintain a heating rate of 0.6 °C (1 °F)/hr. In August 1996, a new program was initiated to determine whether the MSRC aging treatment could be further modified to facilitate its implementation to flight hardware production. It was successfully redesigned into a simplified two-step aging treatment consisting of 132 °C (270 °F)/20 hr + 138 °C (280 °F)/40 hr. Results indicated that two-step aging can achieve the same yield strength levels as those produced by conventional aging while providing greatly improved ductility. Two-step aging proved to be very effective at enhancing CFT, enabling previously rejected materials to meet simulated service requirements. Cryogenic properties are improved by controlling T_1 nucleation and growth so that they are promoted in the matrix and suppressed in the subgrain boundaries.

14. SUBJECT TERMS

multistep heating rate-controlled (MSRC) aging treatment, two-step aging treatment, cryogenic fracture toughness (CFT)

15. NUMBER OF PAGES

28

16. PRICE CODE

17. SECURITY CLASSIFICATION OF REPORT	18. SECURITY CLASSIFICATION OF THIS PAGE	19. SECURITY CLASSIFICATION OF ABSTRACT	20. LIMITATION OF ABSTRACT
Unclassified	Unclassified	Unclassified	Unlimited

National Aeronautics and
Space Administration
AD33
George C. Marshall Space Flight Center
Marshall Space Flight Center, Alabama
35812